Human recombinant FSH induces chemoresistance in human breast cancer cells via HIF-1 alpha activation

HUMAN RECOMBINANT FSH INDUCES CHEMORESISTANCE IN HUMAN BREAST CANCER CELLS VIA HIF-1α ACTIVATION

Bergandi L [a*], Canosa S [b], Pittatore G [b], Silvagno F [a], Doublier S [a], Gennarelli G [b], Benedetto C [b], Revelli A [b]

[a] Department of Oncology, University of Torino, Torino, Italy.

[b] Gynecology and Obstetrics 1, Physiopathology of Reproduction and IVF Unit, Department of Surgical Sciences, S. Anna Hospital, University of Torino, Torino, Italy.

[*] Corresponding author. *Email address:* loredana.bergandi@unito.it
Department of Oncology, University of Torino
Via Santena 5/bis, 10126 Torino, Italy
Phone: +39-011-6705849; fax: +39-011-6705845
e-mail: loredana.bergandi@unito.it

Short title
rhFSH induces chemoresistance in human breast cancer cells

Keywords: recombinant follicle-stimulating hormone, chemoresistance, multidrug resistance, hypoxia-inducible factor 1-alpha, breast cancer cell lines
Funding: This research received no external funding

Disclosure summary
The authors have nothing to disclose

ABSTRACT

Breast cancer patients under 40 years of age who are candidate to chemotherapy with alkylating drugs may undergo controlled ovarian stimulation (COS) with human recombinant follicle-stimulating hormone (rhFSH) in order to get fertility preservation by mature oocyte cryostorage. The direct effect(s) of exogenous rhFSH on the chemosensitivity of breast cancer is currently unknown. To clarify this issue, we incubated four different breast cancer cell lines with rhFSH (10 IU/L, 24h) and then we exposed them to doxorubicin (DOX) or cyclophosphamide (CPA). The effect(s) of rhFSH on human breast cancer cells treated with DOX or CPA was measured in terms of 1) cell viability, 2) cytotoxicity, 3) multidrug resistance (MDR) genes and proteins expression and activities, and 4) hypoxia-inducible factor 1-alpha (HIF-1α) activation. Pre-treatment with rhFSH significantly increased the viability of breast cancer cells after treatment

with DOX or CPA, and reduced the lactate dehydrogenase leakage and reactive oxygen species (ROS) production. Moreover, after pre-incubation with rhFSH, the MDR proteins (Pgp, MPR1 and BCRP) expression and activity resulted up-regulated and the HIF-1α pathway activated. In addition, the use of a widely used HIF-1α inhibitor, the 3-(5'-hydroxymethyl-2'-furyl)-1-benzylindazole (YC-1), prevented the rhFSH effect on the onset of multidrug resistance. Taken together, these observations suggest that a short exposure to rhFSH induces chemoresistance to DOX and CPA in human breast cancer cells via HIF-1α activation.

INTRODUCTION

Breast cancer represents the most frequently diagnosed malignancy in Western countries and the leading cancer-related cause of death worldwide, affecting approximately one out of eight women, many of which still in their reproductive age [1] [2] [3].

Anti-neoplastic drugs (especially alkylating drugs such as cyclophosphamide) represent fundamental tools for breast cancer treatment, but their cytotoxicity involves also the ovary, causing thorough depletion of primordial ovarian follicles, in turn leading to precocious ovarian insufficiency and infertility [4]. This undesired effect is particularly relevant for young women (below 40 years) who are still childless or desire another pregnancy, and, as a consequence, the need to preserve fertility has obtained a growing attention in the last decades, leading to a progressively widespread use of fertility preservation techniques [5].

Currently, fertility preservation includes the pharmacological protection of the ovary by administration of gonadotropin-releasing hormone (GnRH)-analogues, the cryopreservation of mature, unfertilized oocytes and/or embryos, and the cryopreservation of slices of ovarian cortex. Among these options, oocyte cryopreservation is preferred in case of breast cancer because it is a well-established, minimally invasive technique, implies milder bioethical aspects than embryo cryostorage, and, differently from ovarian tissue cryostorage and grafting, bears no risk of reintroducing neoplastic cells [6] [7] [8].

In order to cryopreserve an adequate number of mature oocytes (usually 5-15), Controlled Ovarian Stimulation (COS) is required, accomplished by administering a two-weeks course supraphysiological doses of exogenous follicle-stimulating hormone (FSH), either recombinant or urinary FSH, in the 2–6 weeks interval between surgical removal of breast cancer and initiation of adjuvant chemotherapy [9]. In breast cancer patients (particularly those with estrogen receptors-positive disease), COS generated concerns due to the risk of exposing patients to high estradiol levels (ten folds than normal), that are consequent to multiple follicular development and are known to exert a proliferative effect on estrogen-responsive cells [10] [11]. To minimize the estrogenic effect on estrogen-sensitive cancer cells, selective estrogen receptor inhibitors (e.g. tamoxifen) or aromatase inhibitors (e.g. letrozole) are added to rhFSH [12]. The addition of drugs which counteract the estrogenic effect or avoid excessive E_2 synthesis has been successfully tested in breast cancer patients, and it was proven to be acceptably effective and safe [7] [13] [14].

The attention aimed at controlling the risk of COS for breast cancer patients has been totally focused on the proliferative effect of the high levels of E_2, and not to the potential direct effect(s) of FSH itself. However some data suggest that FSH may exert direct effects on adhesion, motility, and invasion properties of a breast cancer cell line through regulatory actions on the actin cytoskeleton that are not mediated by estrogens [15]. Moreover, Sanchez et al. recently observed in an *in vivo* rat model that gonadotropins may have direct effects on extra-gonadal tissues as different circulating levels of FSH and LH directly correlate with the extent of breast cancer growth [16].

COS for fertility preservation purposes is performed after surgery, but before chemotherapy, and therefore the knowledge on the effect(s) induced by FSH administration on human breast cancer cells is important. In particular, the development of multidrug resistance (MDR) to chemotherapy may result in a significant reduction of therapeutic efficacy and may cause increased risk of tumor persistence/recurrence [17].

Aim of our study was to evaluate the effect(s) of a short exposure of breast cancer cells to exogenous human FSH on their sensitivity/response to the chemotherapeutic drugs DOX and CPA, and the molecular mechanisms underlying this(ese) effect(s).

MATERIALS and METHODS

1. Cells and reagents

Human breast carcinoma cell lines SK-BR-3, MDA-MB-231, MCF-7 and T-47D were obtained from the American Type Culture Collection (Rockville, MD, USA) and grown as a sub-confluent monolayer in humidified incubator at 37°C, 5 % CO_2 and 20 % O_2. The RPMI 1640 medium without phenol red, containing 2 mM L-glutamine, 1% (v/v) antibiotic/antimycotic solution and 10 % (v/v) fetal bovine serum (FBS) was used as culture medium. Before the experiments, cultivated breast cancer cells were kept 24 h in a medium containing 10 % (v/v) steroid-deprived FBS to remove any estrogenic effect from the system.

Unless otherwise specified, reagents were purchased from Sigma Aldrich (Milan, Italy), whereas plastic ware was from Falcon (Beckton Dickinson, Franklin Lakes, NJ).

2. Experimental conditions

Breast cancer cells were incubated for 24 h in the presence or absence (control) of 10 IU/L human recombinant FSH (rhFSH; follitropin-alfa; GONAL-F® (Merck, Darmstadt, Germany), and then were exposed for 24, 48 or 72 h to 2.5-5 µmol/L DOX or 10-40 mM CPA. The concentration of rhFSH, tested directly on the cancer cells, was approximately the one that can be observed in the serum after repeated subcutaneous administration of 150 IU/day Gonal-F® (Laboratoires Merck Serono, Aubonne, Switzerland) over 7 days [18], as COS is usually performed using a rhFSH dose range between 150 and 450 IU/~~ml per~~ day. Moreover, on the basis of preliminary experiments, 10 IU/L FSH was found to be the minimum dose required to show a significant effect on cell proliferation and LDH release. rhLH (Luveris®) (Laboratoires Merck Serono, Aubonne, Switzerland) was used at the dose of 10 IU/L. CPA was chosen as one of the main elective drugs for breast cancer treatment, whereas DOX, used as drug for

solid tumours, was also easily detectable in our experimental approaches and it is often used in studies about chemoresistence.

3. Cell viability

Breast cancer cells were incubated for 24 h in the absence (control) or in the presence of 10 IU/L rhFSH before the chemotherapeutic treatment of 24 and 48 h with DOX (2.5-5 µmol/L) or CPA (10-40 mM), respectively. Then cells were stained for 1h at 37°C in culture medium containing Neutral Red solution, washed three times with phosphate-buffered saline solution (PBS) and rinsed with stop buffer (1:1 of 4.02 g trisodium citrate in 153 mL H_2O, 0.8 mL HCl 0.1 N in 86 mL H_2O and 25 ml of 95 % v/v methanol), as previously described [19]. The absorbance was read at 540 nm and the cell viability was expressed as fold change vs control. Experiments were performed in triplicate and repeated two times.

4. Lactate dehydrogenase (LDH) leakage

Breast cancer cells were incubated for 24 h in the absence (control) or in the presence of 10 IU/L rhFSH before chemotherapeutic treatment, then after 24 and 48 h of incubation with DOX (2.5-5 µmol/L) or CPA (10-40 mM) the extracellular medium was withdrawn and centrifuged at 12,000 g for 30 min to remove cellular debris. Cells were washed with PBS, detached by trypsin/EDTA (0.05/0.02% v/v), resuspended in 1 ml of PBS and sonicated on ice with two 10-s bursts. LDH activity was measured in the extracellular medium and in the cell lysate, as previously described, to verify the cytotoxic effect of chemotherapeutic agents. Both intracellular and extracellular enzyme activities, measured spectrophotometrically as absorbance variation at 340 nm (37 °C), were expressed as nmol NADH oxidized/min/mg cell protein; then extracellular LDH activity was calculated as a ratio to the total (intracellular + extracellular) LDH activity in the dish and expressed as fold change vs control. Experiments were performed in triplicate and repeated three times.

5. Mitochondrial ROS production

Cells were incubated for 24 h in the absence (control) or in the presence of 10 IU/L rhFSH, and then were exposed to 5-10 µM DOX or 25-50 µM CPA for 24 h. Approximately 5×10^6 cells were washed twice in ice-cold PBS and resuspended in 500 µl of mitochondrial lysis buffer A (50 mM Tris, 100 mM KCl, 5 mM MgCl2, 1 mM EDTA, ATP 1.8 mM, pH = 7.2), supplemented with the protease inhibitor cocktail set III (Sigma Aldrich, Milan, Italy), 1 mM phenylmethylsulfonyl fluoride and 2.5 mM sodium fluoride. Samples were clarified by centrifuging at 2,000 rpm for 2 min at 4°C, and the supernatant was collected and centrifuged at 13,000 rpm for 5 min at 4°C. The supernatant (cytosolic fraction) was aliquoted and the pellet containing mitochondria (mitochondrial fraction) was washed in 500 µl buffer A and resuspended in 250 µl mitochondrial resuspension buffer B (250 mM sucrose, 15 mM K_2HPO4, 2 mM MgCl2, 0.5 mM EDTA, 5% w/v BSA). Mitochondrial samples were loaded for 15 min with 10 µM 2′,7′-dichlorodihydrofluorescein diacetate (DCFH-DA), a cell-permeable probe that is cleaved intracellularly by aspecific esterases to form DCFH, which is further oxidized by ROS to form the fluorescent compound dichlorofluorescein (DCF). After the incubation, cells were washed twice with PBS to remove excess probe, and total and mitochondrial DCF fluorescence were determined at an excitation wavelength of 504 nm and an emission wavelength of 529 nm using a Packard EL340 microplate reader (Bio-Tek Instruments, Winooski, VT). The fluorescence value was normalized to the mitochondrial protein content and expressed as fold change vs control [20]. Experiments were performed in triplicate and repeated three times.

6. Doxorubicin accumulation

Cells were incubated for 24 h in the absence (control) or in the presence of 10 IU/L rhFSH, then after exposure to 5-10 µM DOX or 25-50 µM CPA for 24 h they were washed twice in ice-cold PBS and detached with trypsin/EDTA (0.05/0.02% v/v). Cells were centrifuged for 30 sec at 13,000 rpm (4°C) and resuspended in 700 µl of a 1:1 mixture of ethanol plus 0.3 N HCl.

Fifty µl of cell suspension were sonicated on crushed ice with two 10-seconds bursts (Labsonic sonicator, 100 W) and used for measurement of cellular proteins; the remaining part was checked for the DOX content using a Perkin-Elmer LS-5 spectrofluorimeter (Perkin-Elmer). Excitation and emission wavelengths were 475 and 553 nm, respectively. A blank was prepared in the absence of cells in every set of experiments and its fluorescence was subtracted from that obtained in the presence of cells [21]. The fluorescence values were normalized to the protein content and expressed as fold change vs control. Experiments were performed in triplicate and repeated two times.

7. P-glycoprotein 1 (Pgp) and multidrug resistance-associated protein (MRP) activity

The efflux of rhodamine 123, a substrate of Pgp and MRP, was taken as an index measuring Pgp plus MRP activity. Cells were incubated for 24 h without (control) or with 10 IU/L rhFSH, then after wash with fresh PBS they were detached with cell dissociation solution and resuspended at 5×10^5 cells/mL in 1 mL of DMEM medium containing 5% FBS. The samples were maintained at 37° C for 20 min in the presence of 1 µg/mL rhodamine 123. Subsequently, cells were washed and resuspended in 500 µl of PBS, and the intracellular rhodamine content, which is inversely related to its efflux, was detected using a PerkinElmer LS-5 spectrofluorimeter. Excitation and emission wavelengths were 554 and 573 nm, respectively. An aliquot of sample was used for the determination of the intracellular proteins. A blank was prepared in the absence of cells in each set of experiments, and its fluorescence was subtracted from the one measured in each sample [21]. The fluorescence values were normalized to the protein content and expressed as fold change vs control. Experiments were performed in triplicate and repeated two times.

8. Breast cancer resistance protein (BCRP) activity

The efflux of Hoechst 33342, a specific substrate of BCRP, was taken as an index of BCRP activity. Cells were incubated for 24 h in the presence or absence (control) of 10 IU/L rhFSH, then were washed with PBS and resuspended in 500 µL of DPBS buffer (129 mM NaCl, 2.5

mM KCl, 7.4 mM Na_2HPO_4, 1.3 mM KH_2PO_4, 1 mM $CaCl_2$, 0.7 mM $MgSO_4$, 5.3 mM glucose; pH 7.4), in the presence of 50 μM Hoechst 33342 for 15 min at 37° C. Afterwards, 400 μl of stop solution (210 mM KCl, 2 mM Hepes; pH 7.4) was added and cells were lysed with 100 μl of 0.1% v/v Triton-X 100, dissolved in 0.3% v/v NaOH. An aliquot of sample was used for the determination of the intracellular proteins, and the remaining part was analyzed for the Hoechst content, using a PerkinElmer LS-5 spectrofluorimeter. Excitation and emission wavelengths were 370 and 450 nm, respectively. A blank was prepared in the absence of cells in each set of experiments, and its fluorescence was subtracted from the one measured in each sample [21]. The fluorescence values were normalized to the protein content and data were plotted relative to control values. Experiments were performed in triplicate and repeated two times.

9. Western blot analysis

Nuclear extracts (70 μg), obtained with the Nuclear Extraction Kit (Active Motif, Vinci-Biochem, Florence, Italy), were subjected to SDS-PAGE and subsequently transferred to PVDF membrane (Immobilon-P, Millipore, Bedford, MA). The blots were blocked in Tris-buffered saline solution (TBS)-nonfat dry milk 5% for 1 h at room temperature and probed overnight at 4°C with anti-HIF-1α mouse mAb (diluted 1:250 in TBS-nonfat dry milk 5%, cat # 610959, BD Biosciences, San Jose, CA) and anti-PCNA mouse mAb (diluted 1:500 in TBS-nonfat dry milk 5%, sc-56, Santa Cruz Biotechnology, Santa Cruz, CA). The latter antibody was used to check the equal protein loading in nuclear extracts. After an overnight incubation, the membrane was washed with 0.1% v/v TBS-Tween and subjected for 1 h to a peroxidase-conjugated anti-mouse secondary antibody (diluted 1:5000 in 5% w/v PBS-Tween with milk, Bio-Rad Laboratories, Hercules, CA, USA). The membrane was washed again with TBS-Tween, and proteins were detected and quantified by ChemiDoc^{TM} MP System (Bio-Rad Laboratories, Hercules, CA, United States). Densitometric analysis was carried out using ImageJ software (http://rsbweb.nih.gov/ij/).

10. DNA binding enzyme-linked immunosorbent assay (ELISA)

Nuclear extracts (10 μg) obtained with the Nuclear Extraction Kit (Active Motif, Vinci-BiochemSrl, Florence, Italy) were used to detect HIF-1 capacity to bind an HRE by TransAM ELISA Kit (Active Motif, Vinci-BiochemSrl, Florence, Italy), according to the manufacturer's instructions. Briefly, samples were added to a 96-well plate, on which there was an immobilized oligonucleotide containing an HRE (5'-TACGTGCT-3') from the *EPO* gene. They were then incubated with anti-hypoxia-inducible factor 1-alpha (HIF-1α) antibody (diluted 1:1000 in Antibody Binding Buffer), subjected to a horseradish peroxidase-conjugated anti-mouse antibody (diluted 1:1000 in Antibody Binding Buffer) and then incubated with the developing solution, until the blue color development reaction was performed. Absorbance was read on a Packard EL340 microplate reader (Bio-Tek Instruments, Winooski, VT) at 450 nm with a reference wavelength of 655 nm; the absorbance values were expressed as mU optical density/μg nuclear proteins. Experiments were performed in duplicates and repeated three times.

11. Cumulus cells (CCs) collection and mRNA isolation

Cumulus-oocyte complexes (COCs) were retrieved after follicular aspiration in patients undergoing controlled ovarian stimulation for intracytoplasmic sperm injection (ICSI) at the Physiopathology of Reproduction and IVF Unit of S. Anna University Hospital (Torino, Italy), as previously described [22]. Institutional review board approval was obtained from the internal ethical committee which authorized the study. All patients gave written informed consent. Briefly, aspirated follicular fluids were immediately observed under stereomicroscope and COCs were washed in buffered medium (Flushing medium, Cook Ltd, Ireland). Within 4 h from oocyte retrieval CCs were separated by gently pipetting in HEPES-buffered medium containing 80 IU/mL hyaluronidase (Synvitro Hyadase; Origio Medicult, Denmark). Isolated CCs were washed twice in PBS and transferred with ribonuclease inhibitor (Protector RNase Inhibitor, 5 U/liter; Roche Diagnostic, Mannheim, Germany) into a 0.2 ml tube directly plunged in liquid nitrogen and stored at - 80° C until RNA extraction. Cells were lysed using

the Power SYBRGreen Cells-to-CTTM kit (Ambion; Life Technologies Italia, Monza, Italy) and genomic DNA was removed by DNase I.

12. Real-time polymerase chain reaction (qRT-PCR)

Total RNA derived from breast cancer cell line was extracted with TRIzol® (Invitrogen, Thermo Fisher Scientific, Waltham, MA, USA). One μg of total RNA derived from breast cancer cell line and from CCs was reversely transcribed into cDNA at 37°C for 60 min and 95°C for 5 min, in a final volume of 20 μl, using the iScript™ cDNA Synthesis Kit (Biorad, Hercules, CA, USA) according to the manufacturer's instructions. The RT-PCR primers were designed with NCBI Primer-BLAST, synthesized by Sigma (Milan, Italy). was extracted Quantitative PCR was carried out in a final volume of 20 μl using the iTaq™ Universal SYBR® Green Supermix (Biorad, Hercules, CA, USA) with 600 nM specific primers for the quantification of *follicle-stimulating hormone receptor* (FSHR, 5'-CTCACCAAGCTTCGAGTCATCCAA-3' and 5'- AAGGTTGGAGAACACATCTGCCTCT-3'), *luteinizing hormone receptor* (LHR, 5'-GGGCCGAAAACCTTGGAT-3' and 5'-TGAATGGACTCTAGGCCATAGCT-3'), *ATP-binding cassette, sub-family C* (CFTR/MRP) *member 1* (ABCC1) (MRP1, 5'-TCTGGTCAGCCCAACTCTCT-3' and 5'-CCTGTGATCCACCAGAAGGT-3'), *ATP-binding cassette, sub-family C* (CFTR/MRP) *member 5* (ABCC5) (MRP5, 5'- CCCAGGCAACAGAGTCTAACC-3' and 5'-CGGTAATTCAATGCCCAAGTC -3'), *ATP-binding cassette, sub-family C* (CFTR/MRP) *member 8* (ABCC8) (MRP8, 5'- TCTGCGACCTTCTTGTTTGG-3' and 5'-TCAGTACAGCATTTGCAACACTT-3'), *ATP-binding cassette, sub-family G ABCG2* (BCRP, 5'-AGCTGCAAGGAAAGATCCAA-3' and 5'-TCCAGACACACCACGGATAA-3'), *ATP-binding cassette, sub-family B* (MDR/TAP) *member 1* (ABCB1) (Pgp, 5'-GACTGAGCCTGGAGGTGAAG-3' and 5'-CCACCAGAGAGCTGAGTTCC-3'), pyruvate dehydrogenase kinase isozyme 1 (PDK1, 5'-GAAGCAGTTCCTGGACTTCG-3' and 5'-ACCAATTGAACGGATGGTGT-3'), phosphoglycerate kinase 1 (PGK1, 5'-

TCTCATGGATGAGGTGGTGA-3' and 5'-CTTCCAGGAGCTCCAAACTG-3'; vascular endothelial growth factor (VEGF, 5'-ATCTTCAAGCCATCCTGTGTGC-3' and 5'-GCTCACCGCCTCGGCTTGT-3') and *beta 2-microglobulin* (β2M, 5'-AGCAAGGACTGGTCTTTCTATCTC-3' and 5'-ATGTCTCGATCCCACTTAACTA-3') genes. PCR amplification was 1 cycle of denaturation at 95°C for 30 sec, 40 cycles of amplification including denaturation at 95°C for 30 sec and annealing/extension at 60°C for 1 min. Standard curves, with serially diluted solutions (1:1; 1:10; 1:100 and 1:1000 for FSH, BCRP, MRP-1, PDK1, PGK1 and VEGF genes and 1:1; 1:10; 1:100 for LH and Pgp) of cDNAs obtained as a template for each gene, were included in each PCR and amplified by target-specific primer sequence to quantify the PCR baseline subtracted relative fluorescence unit. The threshold cycle (Ct) reflects the cycle number at which the fluorescence generated within a reaction crosses the threshold line. The quantification of each sample was performed comparing each PCR gene product with β2M, used as reference gene to normalize the cDNA in different samples, and expressed in arbitrary units, using the Bio-Rad Software Gene Expression Quantitation (Bio-Rad Laboratories), calculated using the 2_ΔΔCT method [23]. Analyzed transcripts exhibited high linearity amplification plots ($r>0.98$) and similar PCR efficiency (84 % for FSH, LH and MRP1 and VEGF, 95 % for BCRP, PDK1 and PGK1, 83.8 % for Pgp and 94 % for β2M), confirming that the expression of each gene could be directly compared. The specificity of PCRs was confirmed by melting curve analysis. Non-specific amplifications were never detected. Data were plotted relative to control values. Experiments were performed in triplicate and repeated two times.

12. Chromatin immunoprecipitation assay (ChIP)

The chromatin immunoprecipitation assay was done following the recommendations of the manufacturer (Millipore, Merck Spa, Milan, Italy) with some modifications. Briefly, cells were plated in 100-mm diameter dishes (6×10^6 cells per dish), washed twice with 1X PBS, harvested using 1X trypsin and then incubated with formaldehyde (final concentration, 1% v/v)

for 10 min at 37°C with gentle rotating to cross-link proteins to DNA. The cross-linking reaction was stopped by adding glycine to a final concentration of 0.125 M on continue rotating for 5 min and samples were centrifuged at 3.000 *x g* for 1 min at 4 °C. The pellet was resuspended in assay buffer [150 mM NaCl, 1% NP40, 0.5% deoxycholate, 0.1% SDS, 5 mM EDTA, 50 mM Tris-HCl (pH 8.0)] containing 1X protease inhibitor cocktail, 1 mM PMSF, 1 µg/mL aprotinin, and 1 µg/mL pepstatin A. Then, cell lysates were sonicated on ice with a Hielscher UP200S ultrasound sonicator (3 × 60 s, amplitude 40 %; Hielscher Ultrasonics GmbH, Germany) until cross-linked chromatins were sheared to yield DNA fragments between 200 and 1.000 bp. Samples were centrifuged for 15 minutes at 4°C. One tenth of whole lysate was used to quantify the amount of DNA present in different samples and considered as "input DNA". Supernatants were incubated 30 minutes at 4°C with Protein A agarose/sperm DNA (50% slurry) in agitation to reduce non-specific background. Immunoprecipitation was then done overnight at 4°C with 5 µg of anti-HIF-1α antibody [rabbit polyclonal, (H-206): sc-10790, Santa Cruz Biotechnology, Texas, USA] or with rabbit IgG (2729: Cell Signalling Technology, Danvers, MA 01923, USA), used as negative control. The supernatants were then supplemented with 5 M NaCl and heated overnight at 65°C to reverse protein-DNA cross-links. The immunocomplexes were further treated with DNase-and RNase-free proteinase K. DNA was purified by phenol/chloroform extraction and ethanol precipitation, and the yield of target region DNA in each sample after ChIP was analyzed by quantitative PCR with specific primers flanking the putative HRE within the promoter region of the human PDK1 gene (named "PDK1+", p1 primer: 5'-GGTCTCCTGTCTCCCTGTAT-3'; p2 primer: 5'-CTTGACAAGGTTGAGGACGC-3'), primers flanking a PDK1 promoter region that does not contain HRE (named " PDK1-", used as a negative control, p1 primer: 5'-GATTGGGAGGGCAGAGGAAG-3'; p2 primer: 5'-GTCGGGTGATGGGACTGG-3'), primers flanking the HRE of PGK1 promoter (named " PGK1+", p1 primer: 5'-GATCTTCGCCGCTACCCTT-3'; p2 primer: 5'-GCGAGGGTACTAGTGAGACG-3'),

primers flanking a PGK1 promoter region that does not contain HRE (named "PGK1-", used as a negative control, p1 primer: 5'-GCAGCCTCGAATTCCACG-3'; p2 primer: 5'-AAGAATGTGCGAGACCCAGG-3'), primers flanking the HRE of VEGF promoter (used as a positive control, p1 primer: 5'- GTGTGTCCCTCTCCCCAC-3'; p2 primer: 5'-GGGAGCAGGAAAGTGAGGTT-3') and primers flanking a VEGF promoter region that does not contain HRE (named "PGK1-", used as a negative control, p1 primer: 5'-ACAGGGAAGCTGGGTGAATG-3'; p2 primer: 5'- GTGACCCCTGGCCTTCTC-3').

Cycling was: 1 cycle of denaturation at 95°C for 30 sec, 40 cycles of amplification including denaturation at 95°C for 30 sec and annealing/extension at 60°C for 1 min.

Standard curves, with serially diluted solutions (1:1; 1:10; 1:100 and 1:1000 for PDK1+, PGK1+ and VEGF+ genes) of cDNAs obtained as a template for each gene, were included in each PCR and amplified by target-specific primer sequence to quantify the PCR baseline subtracted relative fluorescence unit. Analyzed transcripts exhibited high linearity amplification plots ($r > 0.97$) and similar PCR efficiency (85% for PDK1 and for VEGF, 91% for PGK and 94% for β2M), confirming that the expression of each gene could be directly compared. Data were plotted relative to control values. Experiments were performed in two times.

13. Statistical analysis

Data were expressed as mean ± SEM. The results were checked for normal distribution and analyzed by one-way analysis of variance (ANOVA) followed by Tukey's test. Statistical significance level was set at $p=0.05$.

RESULTS

rhFSH effect on DOX- or CPA-induced cytotoxicity

Cultured cells of the human breast carcinoma cell lines SK-BR-3, MDA-MB-231, MCF-7 and T-47D were treated with different concentrations of DOX (2.5-5 μM) or CPA (10-40 nM) for 24, 48, and 72 hours in order to cell viability. The treatment resulted in a dose-dependent

decrease of cell viability measured by neutral red uptake assay, and different cell lines showed different sensibility to DOX and CPA: T-47D cell survival was only partially affected by DOX and CPA at the administered doses, whereas cell viability was significantly reduced when the other three cell lines were tested (Figure 1, A and B). Pre-treatment for 24 h with 10 IU/L rhFSH significantly ameliorated the cell viability at baseline and after exposure to DOX (Figure 1A) or CPA (Figure 1B) at the same doses and times in all cell lines. As shown in Supplementary Figure 1, SK-BR-3, MDA-MB-231, MCF-7 and T-47D cells expressed both the FSHR and LHR mRNA. Human cumulus cells were used as positive FSHR and LHR expression control. The cell viability data were used to set the experimental conditions of further experiments; the SK-BR-3, MDA-MB-231 and MCF-7cells were treated with drugs at the concentration able to decrease the viability by 50% (3.75 μM for 24 h DOX and 20 nM for 48 h CPA for SK-BR-3 cells, 5 μM for 24 h DOX and 20 nM for 48 h CPA for both MDA-MB-231 and MCF-7 cells) whereas for T-47D cells DOX and CPA were used at the highest dose. In accordance with the results on viability, the extracellular release of the intracellular enzyme LDH, used as an index of cytotoxicity, was significantly lower in SK-BR-3, MDA-MB-231, MCF-7 and T-47D cells after treatment with DOX (Figure 2A) or CPA (Figure 2B) when they were pre-incubated with rhFSH. As both DOX [24] and CPA [25] were shown to display cytotoxic effect via reactive oxygen species (ROS) production, we analyzed the levels of mitochondrial ROS, the main source of cellular ROS. We observed that DOX (Figure 3A) and CPA (Figure 3B) significantly increased mitochondrial ROS production in SK-BR-3, MDA-MB-231 and MCF-7cells, and that rhFSH pre-incubation significantly reduced ROS production. A lower but significant difference in ROS production was observed in T-47D cells, in the presence of DOX or CPA, after pre-incubation with rhFSH (Figure 3A and B). All together our data suggest that FSH reduced the toxicity of the chemotherapeutic drugs by lowering the oxidative damage.

rhFSH effect on ATP binding cassette (ABC) transporters expression and activity

With the aim of testing whether the protecting effect of rhFSH was due to the enhanced drug extrusion promoted by activated MDR proteins, we tested the drug accumulation and the expression and activity of MDR transporters. Upon drug exposure, the amount of intracellular DOX was significantly reduced by 24 h pre-incubation with rhFSH (Figure 4A). Although LH receptor was present in all the tested breast cancer cell lines, the pre-treatment with rhLH (10 IU/L) had no effect on doxorubicin accumulation (Supplementary Figure S2), suggesting that LH it is not able to promote the onset of multidrug resistance increasing the efflux of doxorubicin. Moreover, we observed that the amount of intracellular rhodamine 123 (Figure 4B), an index of Pgp plus MRP activity, and Hoechst 33342 (Figure 4C), an index of BCRP activity, were significantly lower after 24 h pre-incubation with rhFSH. In addition, Pgp, BCRP and MRP1 gene expression (Figure 5) were up-regulated in SK-BR-3, MDA-MB-231 and MCF-7cells after 24 h of incubation with the hormone. These results show that the rhFSH reduced the toxicity of the chemotherapeutic drugs by enhancing their efflux through MDR transporters.

rhFSH effect on HIF-1α activation

Seeking the mechanisms of resistance induced by rhFSH, we tested a central player in MDR and cancer malignity: the hypoxia inducible factor HIF-1α.

We first verified by western blot analysis that HIF-1α was increased in the nucleus of SK-BR-3, MDA-MB-231, MCF-7 and T-47D cells after 24 h of rhFSH treatment under normoxic conditions (Figure 6A and 6B). Moreover, after 24 h of incubation with 10 IU/L rhFSH all the cell lines exhibited an augmented amount of HIF-1α binding to an HRE (Figure 6C). Cell monolayers under hypoxic conditions (3% O_2 for 24 h) and the internal control provided by ELISA kit were used as positive controls (data not shown). Notably, we observed that both the basal level of nuclear HIF-1α and the binding to HRE was significantly higher in T-47D cell lines, in line with their natural chemoresistance demonstrated in our cytotoxicity experiments.

The incubation of cells with a widely used HIF-1α inhibitor, the 3-(5'-hydroxymethyl-2'-furyl)-1-benzylindazole (YC-1) (5 μM for 24 h), which induces a decrease in HIF-1α accumulation by down-regulating HIF-1α mRNA translation [26], significantly decreased HIF-1 capacity of binding to DNA and reverted the effect of the treatment with rhFSH (Figure 6C), thus confirming the soundness of the assay. Moreover, the pre-incubation with rhFSH enhanced the effect of HIF-1 capacity of binding to DNA of both chemotherapeutic agents (Figure 6D, data not shown for CPA as values were superimposable with data obtained in presence of DOX).

ChiP assay was performed to evaluate the occupancy of HIF-1α, and thus its activation, on *PDK1, PGK1* and *VEGF* gene promoters after pre-treatment with rhFSH. We checked in all conditions tested that rhFSH increased the binding of HIF-1α at the *PDK1, PGK1* and *VEGF* than in untreated cells (Figure 7), whereas chromatin precipitated with an anti-HIF-1α antibody showed no enrichment of the *PDK1, PGK1, VEGF* gene promoter region that does not contain a HRE. These results suggest that, after rhFSH stimulation, HIF-1α is recruited to participate to the transcriptional activity of its well-known target genes. These data were confirmed by RT-PCR analysis showing that the expression of the genes PDK1, PGK1, and VEGF was increased in all cells lines after 8 h of incubation with rhFSH (Figure 8), suggesting the rhFSH-mediated functional activation of HIF-1α. Furthermore, the inhibition of HIF-1α by incubating cells with YC-1, an HIF-1α inhibitor, prevented the rhFSH effect both on the doxorubicin accumulation (Figure 9 A) and on the ATP binding cassette (ABC) transporters activities (Figure 9 B and C) in all cell lines, restoring the chemotherapeutic agents levels to a level comparable to the one of control cells. This suggests that HIF-1α blocking rescues the negative effects of FSH on the onset of chemoresistance.

DISCUSSION

Preserving the fertility of female cancer patients in reproductive age (below 40 years) has become a relevant issue in the last decades. In case of breast cancer patients who are candidate to chemotherapy, COS is performed just before chemotherapy; it seems, therefore, quite

relevant to understand whether the exposure to rhFSH could affect the effectiveness of chemotherapy by inducing multidrug resistance (MDR). To the best of our knowledge this issue has never been investigated.

One of the main mechanisms of MDR is the over-expression of ATP-binding cassette (ABC) transporters, such as P-glycoprotein (Pgp) and other MDR-related proteins (e.g. BCRP and MRPs), that actively extrude anticancer drugs from cancer cells [17], lowering the intracellular concentration of chemotherapeutics and consequently causing a reduction of their cytotoxic effect [27] [28] [29]. Also HIF-1α, a central component of hypoxic adaptation, is a crucial factor in MDR: its activation correlates with increased resistance to DOX in cancer cells [27]. Moreover, hypoxia was found to induce expression of BCPR gene in human renal proximal tubular cell line [30], of MRP-1 in colon cancer cells [31], and of MDR1 gene and its product Pgp in transformed epithelia; further, a functional HIF-1α binding site was identified within the BCRP, MRP-1 and MDR1 gene promoters [30] [32], and HIF-1α activation in colon cancer cells was found to increase the expression of Pgp, which in turn decreases the accumulation of intracellular DOX and its cytotoxic effect [28].

In granulosa cells and under normoxic conditions, FSH increases HIF-1α production via stimulation of cAMP and up-regulation of the phosphatidylinositol-3-kinase (PI3K)/Akt/mTOR/HIF-1 pathway [33] [34]. In tumor cells, PI3K/Akt signaling is involved in FSH-induced multiple functions in a FSHR-dependent manner [35]. Indeed, in epithelial ovarian cancer cells FSH may induce proliferation via PI3K/Akt/HIF-1α/cyclin D1 pathway [33] and promote the epithelial-mesenchymal transition, migration and invasion through FSHR-PI3K/Akt-Snail signaling pathway [36]. Moreover, in ovarian serous cystadenocarcinoma HIF1α is involved in FSH-induced VEGF expression [35].

The activation of PI3K/Akt/mTOR pathway, that regulates critical aspects of normal and cancer physiology, including cell proliferation, metabolism, motility, angiogenesis, and apoptosis, is caused either by genetic mutation or amplification and it is also associated with

cancer pathogenesis, progression, and drug resistance [37]. Breast cancer has the highest rate of mutational activation of this pathway (more than 70%) [38] [39].

A widespread expression of FSH receptor (FSHR) was observed in tumor-specific vascular endothelial cells of a wide variety of cancers, including breast cancer [40]. The endothelial expression of FSHR is significantly correlated with the peri-tumoral vessel density and with tumor size, suggesting a direct role of FSH in promoting early tumor angiogenesis [41] [42]. Ji and colleagues found significantly higher levels of mRNA encoding the receptor for FSH in invasive ovarian tumors compared to low malignant tumors and normal in ovary surface epithelium [43]. Moreover, recently, Sellers ZP et al. demonstrated that physiological maternal pituitary sex hormones regulate migration, adhesion and proliferation in early development of embryonic stem cells and teratocarcinoma cells [44]. Also, FSH exerts effects on the FSHR expressed of stem cells located in the ovary surface by undergoing self-renewal, clonal expansion, and initiating neo-oogenesis and primordial follicle assembly. These population of very small embryonic-like stem cells are relatively quiescent and were recently reported to survive chemotherapy and initiate oogenesis in mice when exposed to FSH [45]. Furthermore, the FSH therapy plays a fundamental role in mobilizing very small embryonic-like stem cells and hematopoietic progenitor stem cells into peripheral blood [46]. This suggests that on one hand FSH can become a promising tool in clinical settings, but on the other hand any therapeutic strategies aimed at enhancement of the size of stem/progenitor cell pool by the use of gonadotropin-based therapies should be carefully investigated in terms of clinical safety. Overall, our results show that all the investigated human breast cancer cells express the FSH receptor at the mRNA level and that a short exposure to rFSH is able to induce a significant decrease of intracellular accumulation and cytotoxicity of chemotherapeutic agents DOX and CPA. The signaling of FSH involves the activation of HIF-1α pathway that enhances Pgp, MDR-1 and BCRP expression and activity. The central role of HIF-1α is demonstrated by the reversion of the MDR phenotype exerted by the HIF-1α inhibitor YC-1. Remarkably, our

findings represent the first evidence of a direct role for rFSH in inducing chemoresistance to DOX and CPA in human breast cancer cells via HIF-1α activation.

The concept that COS is a safe procedure for women with breast cancer is based on small and non-randomized observational studies that after a rather short follow-up (7 years) reported a similar survival rate in affected women who underwent COS for fertility preservation vs those who did not [39]. Due to both the extensive intra-individual genetic heterogeneity and the temporal heterogeneity reflecting variability over time during tumor growth and development or in response to treatment [47], high quality evidence of COS safety in breast cancer patients is difficult to obtain. In this contest, our in vitro research can provide suggestions for future case-control studies or for larger scale trials focused on women with breast cancer seeking fertility preservation before undergoing chemotherapy.

LEGENDS of SUPPLEMENTARY FIGURES

Figure S1. FSHR and LHR mRNA levels in breast cancer cells (lines SK-BR-3, MDA-MB-231, MCF-7 and T-47D). Cells were analyzed by quantitative real-time polymerase chain reaction (RT-qPCR). Measurements (n = 4) were performed in duplicate and repeated two times, and data, expressed as relative expression versus human cumulus cells (positive control), are presented as means ± SEM.* $p< 0.01$, ** $p< 0.001$ and *** $p< 0.0001$ vs control (cumuls cells).

Figure S2. Effect of rhLH on intracellular DOX accumulation in breast cancer cells (lines SK-BR-3, MDA-MB-231, MCF-7 and T-47D). Cells were cultured for 24 h in the absence or presence of 10 IU/L rhLH, then were incubated for other 24 h in the presence of different concentrations (3.75 or 5 μM) of DOX. For DOX accumulation assay, measurements were performed in triplicate and repeated two times (n = 6) and data were represented as fold change vs control (means ± SEM).

Author contributions:

Conceptualization, Alberto Revelli;
Methodology, Loredana Bergandi and Stefano Canosa;
Project administration, Loredana Bergandi;
Data curation, Loredana Bergandi and Gianluca Gennarelli;
Visualization, Giulia Pittatore;
Formal analysis, Loredana Bergandi;
Validation, Loredana Bergandi, Francesca Silvagno and Sophie Doublier;
Supervision, Alberto Revelli and Chiara Benedetto;
Writing – original draft, Loredana Bergandi and Alberto Revelli;
Final editing, Francesca Silvagno, Giulia Pittatore and Stefano Canosa.

All authors have read the manuscript and approved its submission to Biology of Reproduction.

ORCID ID:
Loredana Bergandi 0000-0003-0951-7340
Stefano Canosa 0000-0001-6402-6750
Francesca Silvagno 0000-0002-8800-9135
Sophie Doublier 0000-0002-7335-5801
Giulia Pittatore 0000-0002-2124-7075
Gennarelli Gianluca 0000-0003-4390-9428
Chiara Benedetto 0000-0003-1514-4771
Alberto Revelli 0000-0002-5797-3722
Funding: This research received no external funding

Acknowledgments: This work was supported by MIUR in the PhD (for S.C. and G.P.) and Post-doc Program (for L.B.) of the University of Torino.

Conflicts of Interest: The authors declare no conflict of interest

REFERENCES

[1] Global Cancer Observatory. http://gco.iarc.fr/. Accessed 11 August 2018.
[2] Jemal A, Center MM, DeSantis C, Ward EM. Global patterns of cancer incidence and mortality rates and trends. Cancer Epidemiol Biomark Prev Publ Am Assoc Cancer Res Cosponsored Am Soc Prev Oncol 2010; 19:1893–1907.
[3] Oktay K, Harvey BE, Partridge AH, Quinn GP, Reinecke J, Taylor HS, Wallace WH, Wang ET, Loren AW. Fertility Preservation in Patients With Cancer: ASCO Clinical Practice Guideline Update. J Clin Oncol Off J Am Soc Clin Oncol 2018; 36:1994–2001.
[4] Molina JR, Barton DL, Loprinzi CL. Chemotherapy-induced ovarian failure: manifestations and management. Drug Saf 2005; 28:401–416.
[5] Kim S-Y, Kim SK, Lee JR, Woodruff TK. Toward precision medicine for preserving fertility in cancer patients: existing and emerging fertility preservation options for women. J Gynecol Oncol 2016; 27:e22.
[6] Kasum M, von Wolff M, Franulić D, Čehić E, Klepac-Pulanić T, Orešković S, Juras J. Fertility preservation options in breast cancer patients. Gynecol Endocrinol Off J Int Soc Gynecol Endocrinol 2015; 31:846–851.
[7] Revelli A, Porcu E, Levi Setti PE, Delle Piane L, Merlo DF, Anserini P. Is letrozole needed for controlled ovarian stimulation in patients with estrogen receptor-positive breast cancer? Gynecol Endocrinol Off J Int Soc Gynecol Endocrinol 2013; 29:993–996.
[8] Revelli A, Molinari E, Salvagno F, Delle Piane L, Dolfin E, Ochetti S. Oocyte cryostorage to preserve fertility in oncological patients. Obstet Gynecol Int 2012; 2012:525896.
[9] Campos JR, Rosa-E-Silva ACJ de S. Cryopreservation and fertility: current and prospective possibilities for female cancer patients. ISRN Obstet Gynecol 2011; 2011:350813.
[10] Cavagna F, Pontes A, Cavagna M, Dzik A, Donadio NF, Portela R, Nagai MT, Gebrim LH. A specific controlled ovarian stimulation (COS) protocol for fertility preservation in women with breast cancer undergoing neoadjuvant chemotherapy. Contemp Oncol Poznan Pol 2017; 21:290–294.
[11] Chen C-L, Cheung LWT, Lau M-T, Choi J-H, Auersperg N, Wang H-S, Wong AST, Leung PCK. Differential role of gonadotropin-releasing hormone on human ovarian epithelial cancer cell invasion. Endocrine 2007; 31:311–320.
[12] Meirow D, Raanani H, Maman E, Paluch-Shimon S, Shapira M, Cohen Y, Kuchuk I, Hourvitz A, Levron J, Mozer-Mendel M, Brengauz M, Biderman H, et al. Tamoxifen co-administration during controlled ovarian hyperstimulation for in vitro fertilization in breast cancer patients

increases the safety of fertility-preservation treatment strategies. Fertil Steril 2014; 102:488-495.e3.
[13] Kim SS, Klemp J, Fabian C. Breast cancer and fertility preservation. Fertil Steril 2011; 95:1535–1543.
[14] Dahhan T, Balkenende EME, Beerendonk CCM, Fleischer K, Stoop D, Bos AME, Lambalk CB, Schats R, van Golde RJT, Schipper I, Louwé LA, Cantineau AEP, et al. Stimulation of the ovaries in women with breast cancer undergoing fertility preservation: Alternative versus standard stimulation protocols; the study protocol of the STIM-trial. Contemp Clin Trials 2017; 61:96–100.
[15] Sanchez AM, Flamini MI, Russo E, Casarosa E, Pacini S, Petrini M, Genazzani AR, Simoncini T. LH and FSH promote migration and invasion properties of a breast cancer cell line through regulatory actions on the actin cytoskeleton. Mol Cell Endocrinol 2016; 437:22–34.
[16] Sanchez AM, Flamini MI, Zullino S, Russo E, Giannini A, Mannella P, Naccarato AG, Genazzani AR, Simoncini T. Regulatory Actions of LH and Follicle-Stimulating Hormone on Breast Cancer Cells and Mammary Tumors in Rats. Front Endocrinol 2018; 9:239.
[17] Gottesman MM. Mechanisms of cancer drug resistance. Annu Rev Med 2002; 53:615–627.
[18] Porchet HC, le Cotonnec JY, Loumaye E. Clinical pharmacology of recombinant human follicle-stimulating hormone. III. Pharmacokinetic-pharmacodynamic modeling after repeated subcutaneous administration. Fertil Steril 1994; 61:687–695.
[19] Gelsomino G, Corsetto PA, Campia I, Montorfano G, Kopecka J, Castella B, Gazzano E, Ghigo D, Rizzo AM, Riganti C. Omega 3 fatty acids chemosensitize multidrug resistant colon cancer cells by down-regulating cholesterol synthesis and altering detergent resistant membranes composition. Mol Cancer 2013; 12:137.
[20] Bergandi L, Aina V, Garetto S, Malavasi G, Aldieri E, Laurenti E, Matera L, Morterra C, Ghigo D. Fluoride-containing bioactive glasses inhibit pentose phosphate oxidative pathway and glucose 6-phosphate dehydrogenase activity in human osteoblasts. Chem Biol Interact 2010; 183:405–415.
[21] Riganti C, Voena C, Kopecka J, Corsetto PA, Montorfano G, Enrico E, Costamagna C, Rizzo AM, Ghigo D, Bosia A. Liposome-encapsulated doxorubicin reverses drug resistance by inhibiting P-glycoprotein in human cancer cells. Mol Pharm 2011; 8:683–700.
[22] Bergandi L, Basso G, Evangelista F, Canosa S, Dalmasso P, Aldieri E, Revelli A, Benedetto C, Ghigo D. Inducible nitric oxide synthase and heme oxygenase 1 are expressed in human cumulus cells and may be used as biomarkers of oocyte competence. Reprod Sci Thousand Oaks Calif 2014; 21:1370–1377.
[23] Livak KJ, Schmittgen TD. Analysis of relative gene expression data using real-time quantitative PCR and the 2(-Delta Delta C(T)) Method. Methods San Diego Calif 2001; 25:402–408.
[24] Carlisi D, De Blasio A, Drago-Ferrante R, Di Fiore R, Buttitta G, Morreale M, Scerri C, Vento R, Tesoriere G. Parthenolide prevents resistance of MDA-MB231 cells to doxorubicin and mitoxantrone: the role of Nrf2. Cell Death Discov 2017; 3:17078.
[25] Kaufmann M, Hortobagyi GN, Goldhirsch A, Scholl S, Makris A, Valagussa P, Blohmer J-U, Eiermann W, Jackesz R, Jonat W, Lebeau A, Loibl S, et al. Recommendations from an international expert panel on the use of neoadjuvant (primary) systemic treatment of operable breast cancer: an update. J Clin Oncol Off J Am Soc Clin Oncol 2006; 24:1940–1949.
[26] Sun H-L, Liu Y-N, Huang Y-T, Pan S-L, Huang D-Y, Guh J-H, Lee F-Y, Kuo S-C, Teng C-M. YC-1 inhibits HIF-1 expression in prostate cancer cells: contribution of Akt/NF-κB signaling to HIF-1α accumulation during hypoxia. Oncogene 2007; 26:3941–3951.
[27] Riganti C, Doublier S, Aldieri E, Orecchia S, Betta PG, Gazzano E, Ghigo D, Bosia A. Asbestos induces doxorubicin resistance in MM98 mesothelioma cells via HIF-1alpha. Eur Respir J 2008; 32:443–451.

[28] Riganti C, Doublier S, Viarisio D, Miraglia E, Pescarmona G, Ghigo D, Bosia A. Artemisinin induces doxorubicin resistance in human colon cancer cells via calcium-dependent activation of HIF-1alpha and P-glycoprotein overexpression. Br J Pharmacol 2009; 156:1054–1066.
[29] Doublier S, Belisario DC, Polimeni M, Annaratone L, Riganti C, Allia E, Ghigo D, Bosia A, Sapino A. HIF-1 activation induces doxorubicin resistance in MCF7 3-D spheroids via P-glycoprotein expression: a potential model of the chemo-resistance of invasive micropapillary carcinoma of the breast. BMC Cancer 2012; 12:4.
[30] Nishihashi K, Kawashima K, Nomura T, Urakami-Takebayashi Y, Miyazaki M, Takano M, Nagai J. Cobalt Chloride Induces Expression and Function of Breast Cancer Resistance Protein (BCRP/ABCG2) in Human Renal Proximal Tubular Epithelial Cell Line HK-2. Biol Pharm Bull 2017; 40:82–87.
[31] Lv Y, Zhao S, Han J, Zheng L, Yang Z, Zhao L. Hypoxia-inducible factor-1α induces multidrug resistance protein in colon cancer. OncoTargets Ther 2015; 8:1941–1948.
[32] Comerford KM, Wallace TJ, Karhausen J, Louis NA, Montalto MC, Colgan SP. Hypoxia-inducible factor-1-dependent regulation of the multidrug resistance (MDR1) gene. Cancer Res 2002; 62:3387–3394.
[33] Alam H, Maizels ET, Park Y, Ghaey S, Feiger ZJ, Chandel NS, Hunzicker-Dunn M. Follicle-stimulating hormone activation of hypoxia-inducible factor-1 by the phosphatidylinositol 3-kinase/AKT/Ras homolog enriched in brain (Rheb)/mammalian target of rapamycin (mTOR) pathway is necessary for induction of select protein markers of follicular differentiation. J Biol Chem 2004; 279:19431–19440.
[34] Alam H, Weck J, Maizels E, Park Y, Lee EJ, Ashcroft M, Hunzicker-Dunn M. Role of the phosphatidylinositol-3-kinase and extracellular regulated kinase pathways in the induction of hypoxia-inducible factor (HIF)-1 activity and the HIF-1 target vascular endothelial growth factor in ovarian granulosa cells in response to follicle-stimulating hormone. Endocrinology 2009; 150:915–928.
[35] Huang Y, Hua K, Zhou X, Jin H, Chen X, Lu X, Yu Y, Zha X, Feng Y. Activation of the PI3K/AKT pathway mediates FSH-stimulated VEGF expression in ovarian serous cystadenocarcinoma. Cell Res 2008; 18:780–791.
[36] Yang Y, Zhang J, Zhu Y, Zhang Z, Sun H, Feng Y. Follicle-stimulating hormone induced epithelial-mesenchymal transition of epithelial ovarian cancer cells through follicle-stimulating hormone receptor PI3K/Akt-Snail signaling pathway. Int J Gynecol Cancer Off J Int Gynecol Cancer Soc 2014; 24:1564–1574.
[37] O'Shaughnessy J, Thaddeus Beck J, Royce M. Everolimus-based combination therapies for HR+, HER2- metastatic breast cancer. Cancer Treat Rev 2018; 69:204–214.
[38] Bachelot T, Bourgier C, Cropet C, Ray-Coquard I, Ferrero J-M, Freyer G, Abadie-Lacourtoisie S, Eymard J-C, Debled M, Spaëth D, Legouffe E, Allouache D, et al. Randomized phase II trial of everolimus in combination with tamoxifen in patients with hormone receptor-positive, human epidermal growth factor receptor 2-negative metastatic breast cancer with prior exposure to aromatase inhibitors: a GINECO study. J Clin Oncol Off J Am Soc Clin Oncol 2012; 30:2718–2724.
[39] Rodgers RJ, Reid GD, Koch J, Deans R, Ledger WL, Friedlander M, Gilchrist RB, Walters KA, Abbott JA. The safety and efficacy of controlled ovarian hyperstimulation for fertility preservation in women with early breast cancer: a systematic review. Hum Reprod Oxf Engl 2017; 32:1033–1045.
[40] Pawlikowski Łódź M. Expression of follicle stimulating hormone receptors in intra-tumoral vasculature and in tumoral cells - the involvement in tumour progression and the perspectives of application in cancer diagnosis and therapy. Endokrynol Pol 2018; 69:192–198.
[41] Gloaguen P, Crépieux P, Heitzler D, Poupon A, Reiter E. Mapping the follicle-stimulating hormone-induced signaling networks. Front Endocrinol 2011; 2:45.

[42] Planeix F, Siraj M-A, Bidard F-C, Robin B, Pichon C, Sastre-Garau X, Antoine M, Ghinea N. Endothelial follicle-stimulating hormone receptor expression in invasive breast cancer and vascular remodeling at tumor periphery. J Exp Clin Cancer Res CR 2015; 34:12.
[43] Ji Q, Liu PI, Chen PK, Aoyama C. Follicle stimulating hormone-induced growth promotion and gene expression profiles on ovarian surface epithelial cells. Int J Cancer 2004; 112:803–814.
[44] Sellers ZP, Bujko K, Schneider G, Kucia M, Ratajczak MZ. Novel evidence that pituitary sex hormones regulate migration, adhesion, and proliferation of embryonic stem cells and teratocarcinoma cells. Oncol Rep 2018; 39:851–859.
[45] Bhartiya D, Parte S, Patel H, Sriraman K, Zaveri K, Hinduja I. Novel Action of FSH on Stem Cells in Adult Mammalian Ovary Induces Postnatal Oogenesis and Primordial Follicle Assembly. Stem Cells Int 2016; 2016:5096596.
[46] Zbucka-Kretowska M, Eljaszewicz A, Lipinska D, Grubczak K, Rusak M, Mrugacz G, Dabrowska M, Ratajczak MZ, Moniuszko M. Effective Mobilization of Very Small Embryonic-Like Stem Cells and Hematopoietic Stem/Progenitor Cells but Not Endothelial Progenitor Cells by Follicle-Stimulating Hormone Therapy. Stem Cells Int 2016; 2016:8530207.
[47] Ellsworth RE, Blackburn HL, Shriver CD, Soon-Shiong P, Ellsworth DL. Molecular heterogeneity in breast cancer: State of the science and implications for patient care. Semin Cell Dev Biol 2017; 64:65–72.

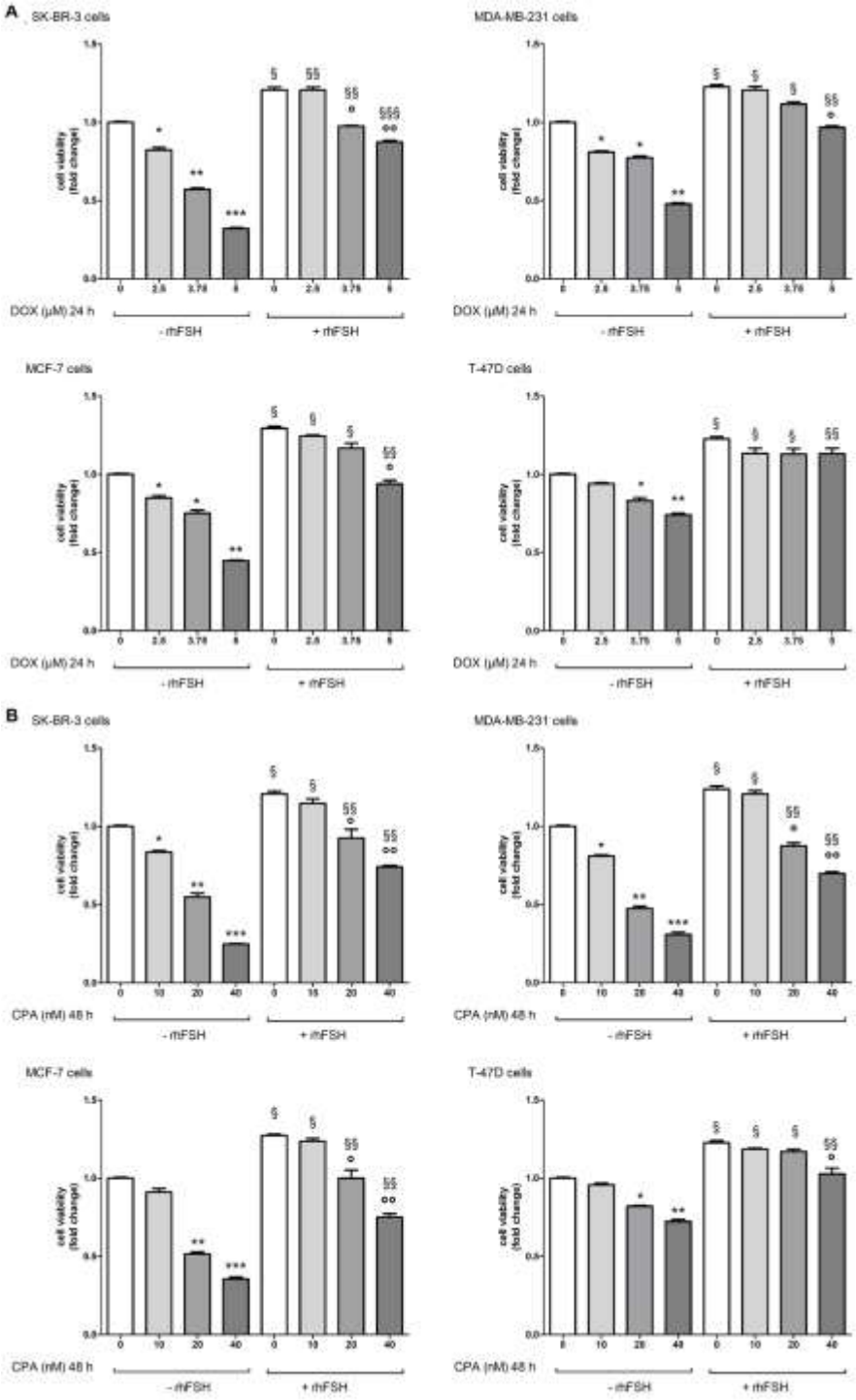

Figure 1. Effect of rhFSH on cell viability after chemotherapeutic treatment of four human breast cancer cell lines. SK-BR-3, MDA-MB-231, MCF-7 and T-47D cells were cultured for 24 h in the absence or presence of 10 IU/L rhFSH, then were left untreated or incubated for 24 h in the presence of different concentrations (2.5, 3.75 or 5μM) of DOX (Panel A) or different concentrations (10, 20 or 40 mM) of CPA (Panel B). Cell viability was evaluated by neutral red staining, carried out in triplicate and repeated two times (n= 6). Data were represented as fold change vs control without rhFSH pre-incubation (means ± SEM). *p< 0.01, **p< 0.001 and ***p< 0.0001 vs control (0 μM DOX or CPA) without rhFSH pre-incubation; °p< 0.01 and °°p< 0.001 vs control (0 μM DOX or CPA) after rhFSH pre-incubation; § p< 0.01, §§ p< 0.001 and §§§ p< 0.0001 vs the same treatment without rhFSH pre-incubation.

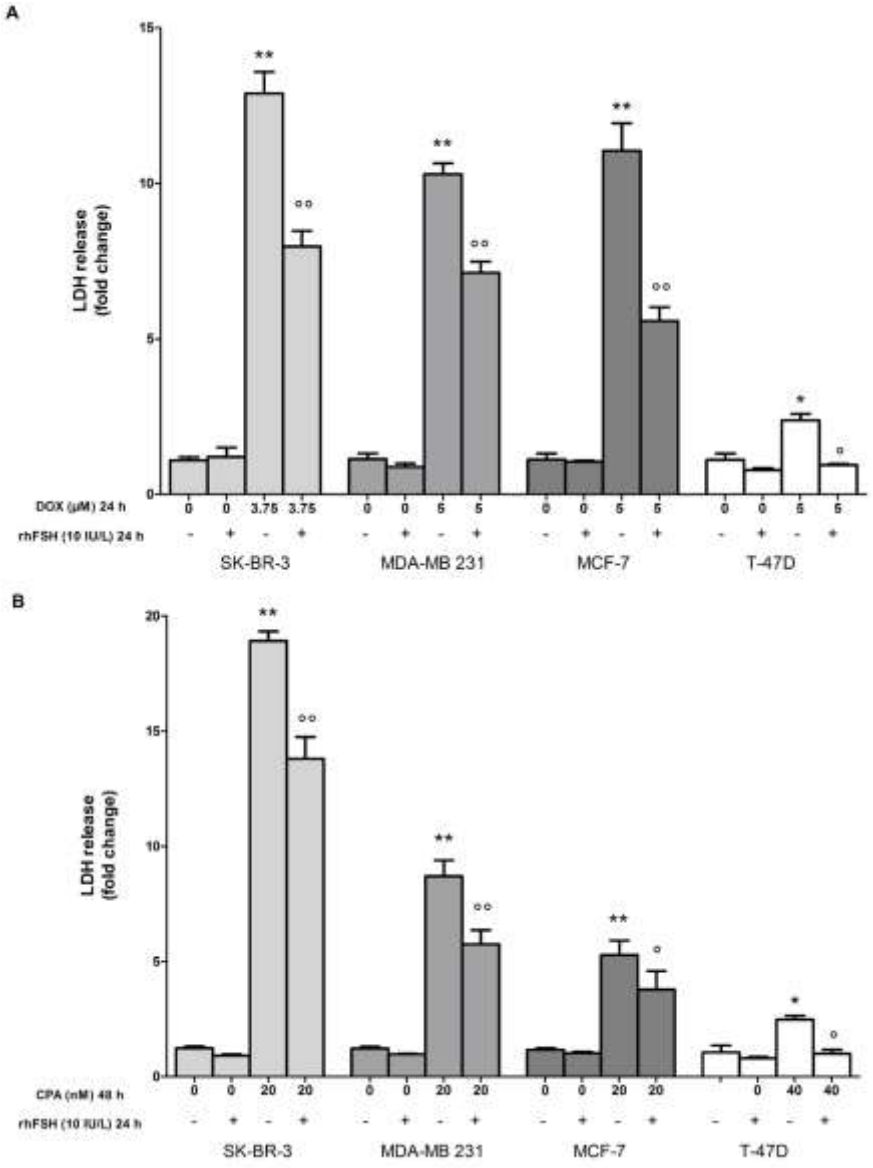

Figure 2. Effect of rhFSH on LDH release after chemotherapeutic treatment of four human breast cancer cell lines.

SK-BR-3, MDA-MB-231, MCF-7 and T-47D cells were exposed to 24 h pre-incubation with 10 IU/L rhFSH or left untreated, then were incubated for 24 h with different concentrations (3.75 or 5μM) of DOX or different doses (20 or 40 nM) of CPA. LDH release was calculated as extracellular vs total (intracellular and extracellular) LDH activity in the dish. Measurements were carried out in triplicate and repeated three times; data were represented as fold change vs respective control (means ± SEM). *p< 0.01, **p< 0.001 vs control (0 μM DOX or CPA) without rhFSH pre-incubation; °p< 0.01 and °°p< 0.001 vs control (0 μM DOX or CPA) after rhFSH pre-incubation.

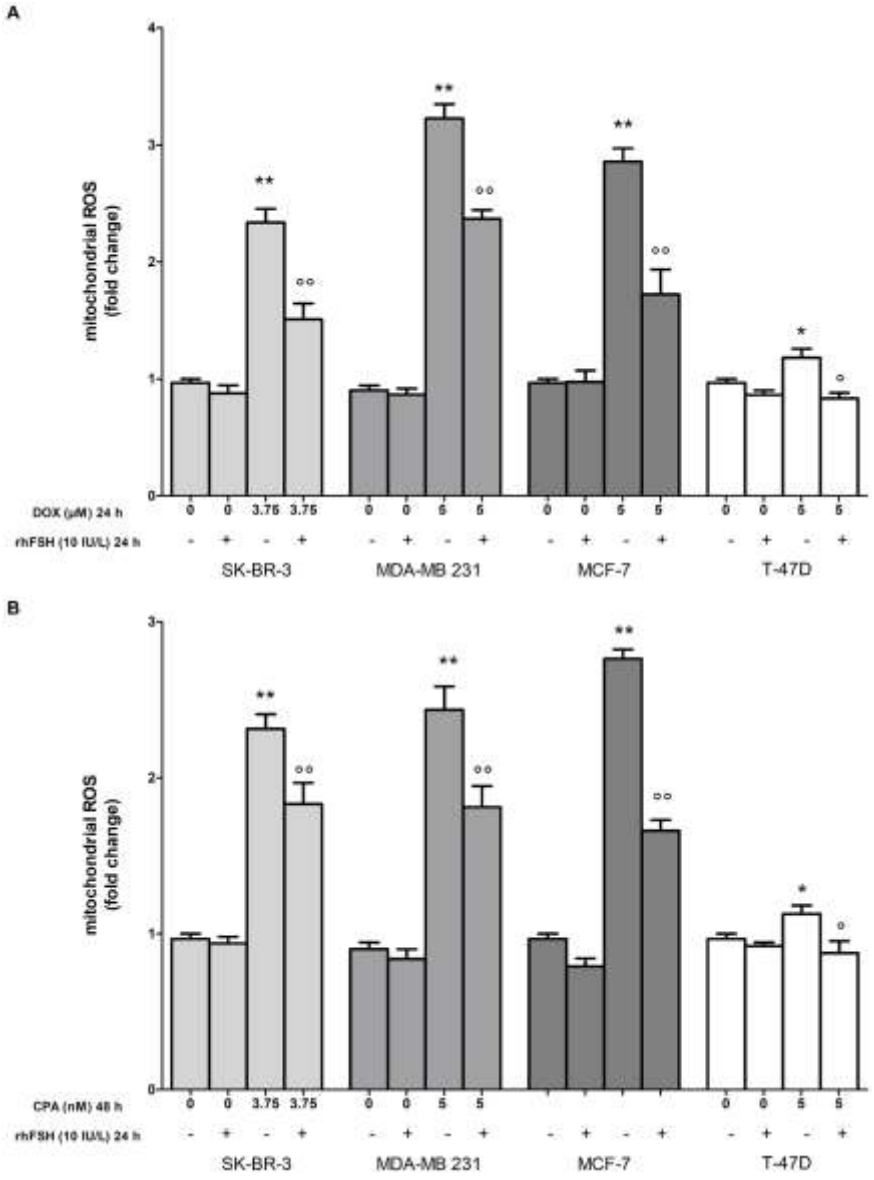

Figure 3. Effect of rhFSH on mitochondrial ROS production after chemotherapeutic treatment of four human breast cancer cell lines. Cells were exposed to 24 h pre-incubation with 10 IU/L rhFSH or left untreated, then were treated with different concentrations (3.75 or 5μM) of DOX or CPA (20 or 40 nM). The mitochondrial levels of ROS were measured fluorimetrically using the DCFDA-AM probe. The assay was carried out in triplicate and repeated two times (n = 6) Data were represented as fold change vs respective control (means ± SEM). *p< 0.01, **p< 0.001 vs control (0 μM DOX or CPA) without rhFSH pre-incubation; °p< 0.01 and °°p< 0.001 vs control (0 μM DOX or CPA) after rhFSH pre-incubation

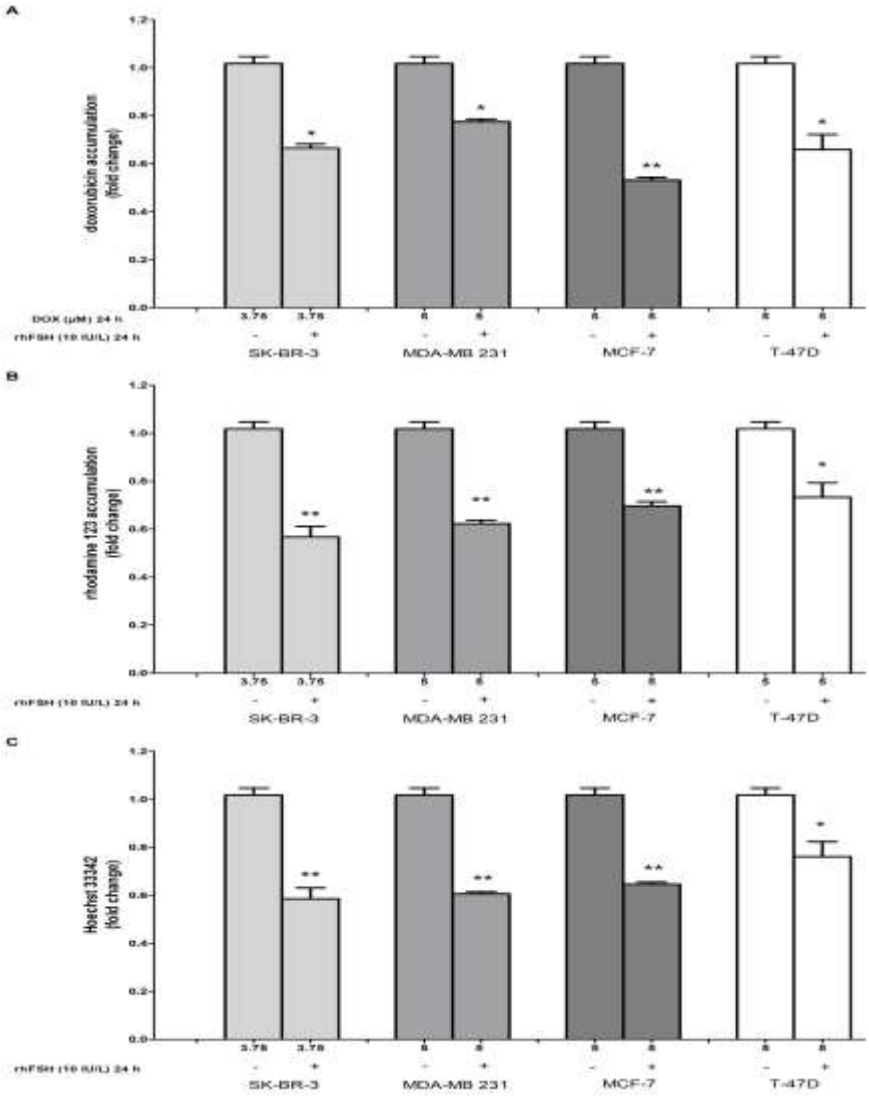

Figure 4. Effect of rhFSH on intracellular DOX accumulation and transporter activity after chemotherapeutic treatment of four human breast cancer cell lines. Effect of 24 h pre-incubation with rhFSH on intracellular DOX accumulation (Panel A) and on the ATP binding cassette transporters activity (Panel B and C) in breast cancer cells (lines SK-BR-3, MDA-MB-231, MCF-7 and T-47D). Cells were cultured for 24 h in the absence or presence of 10 IU/L rhFSH, then were incubated for other 24 h in the presence of different concentrations (3.75 or 5 μM) of DOX. Measurements were performed in triplicate and repeated two times (n = 6) and data were represented as fold change vs control. (A) For DOX accumulation assay, intracellular doxo was measured at the spectrofluorimeter. For ATP binding cassette transporters activity assays, the cells were cultured for 24 h in the presence of 10 IU/L rhFSH, then were washed and maintained for further 20 min at 37°C in medium containing the substrate of different transporters: (B) rhodamine 123 to assess Pgp and MRP activity (C) Hoechst 33342 to assess BCRP activity. Then cells were lysed and the intracellular fluorescence, inversely related to fluorescence efflux, was assessed fluorimetrically. Measurements were performed in triplicate and repeated two times (n = 6). The absorbance values of the treated cells are expressed as fold change vs control (means ± SEM). * $p < 0.01$ and ** $p < 0.001$ in presence of 10 IU/L rhFSH vs absence of rhFSH.

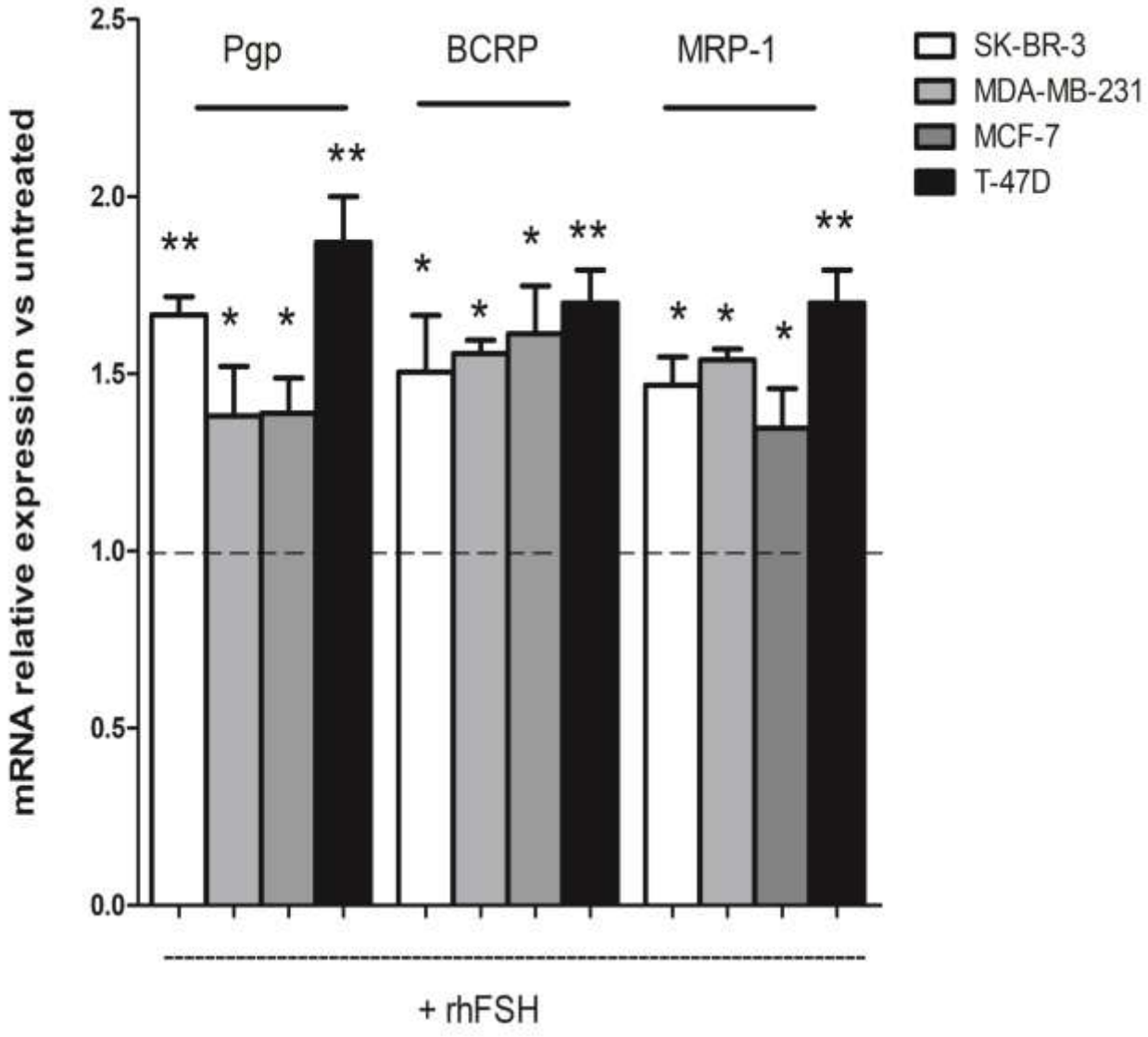

Figure 5. Effect rhFSH on mRNA levels of MDR-related proteins (BCRP and MRP1) and P-glycoprotein (Pgp) genes in human breast cancer cells (lines).

SK-BR-3, MDA-MB-231, MCF-7 and T-47D cells were cultured for 24 h in the absence or presence of 10 IU/L of rhFSH, then were analyzed by quantitative real-time polymerase chain reaction (RT-qPCR). Measurements (n = 6) were performed in triplicate and repeated two times, and data, expressed as relative expression vs respective control in the absence of rhFSH pre-incubation (untreated, represented as dot line), are presented as means ± SEM.* $p < 0.01$ and ** $p < 0.001$ after rhFSH pre-incubation vs absence of rhFSH.

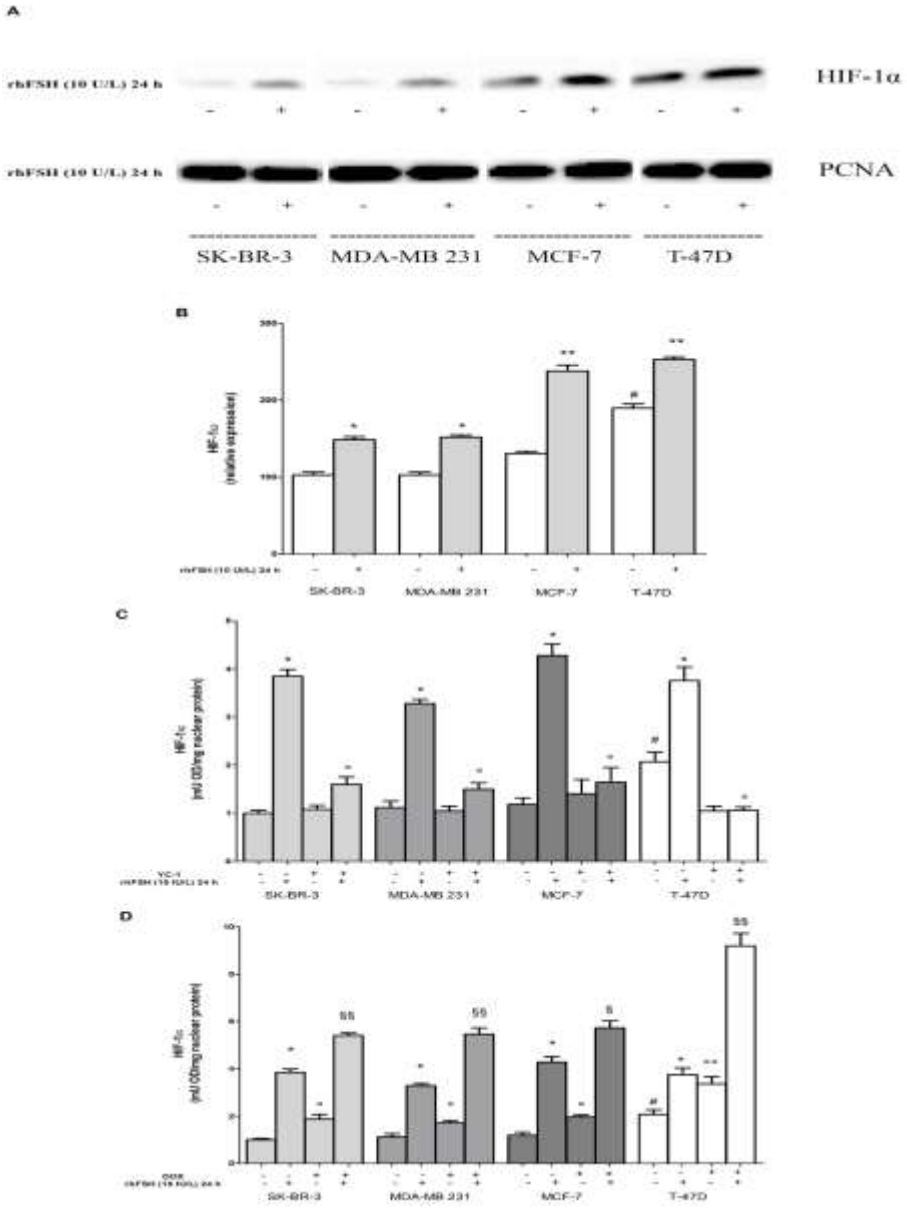

Figure 6. Effects of rhFSH on HIF-1α nuclear traslocation and DNA binding in human breast cancer cells (lines SK-BR-3, MDA-MB-231, MCF-7 and T-47D). (A) Representative gel of Western blot analysis of HIF-1α performed on nuclear extracts. This figure is representative of two similar experiments. The level of proliferating cell nuclear antigen (PCNA) was used to check the equal protein loading. (B) Bands from two independent experiments were quantified, normalized for loading as a ratio to PCNA expression and data plotted on graph relative to control SK-BR-3 (the weakest expression). Data are presented as means ± SEM. *p< 0.01 and **p< 0.001 vs absence of rhFSH; # p< 0.001 vs SK-BR-3, MDA-MB231 and MCF-7 untreated. (C) Detection of HIF-1α DNA binding. Cells were pre-incubated in the absence (-) or in the presence (+) of 5 μM YC-1 for 24 h and then incubated with rhFSH for 24 h. The figure is representative of three experiments performed in duplicate.* p< 0.001 compared to untreated; ° p< 0.001 rhFSH with YC-1 vs rhFSH without YC-1; # p< 0.001 vs SK-BR-3, MDA-MB231 and MCF-7 untreated. (D) Detection of HIF-1α DNA binding. Cells were pre-incubated in the absence (-) or in the presence (+) of 5 μM DOX and with or without of rhFSH for 24 h. The figure is representative of three experiments performed in duplicate. * p< 0.001 vs untreated; ° p< 0.001 vs untreated; § p< 0.01 and §§ p< 0.001 vs rhFSH in absence of DOX; # p< 0.001 vs SK-BR-3, MDA-MB231 and MCF-7 untreated.

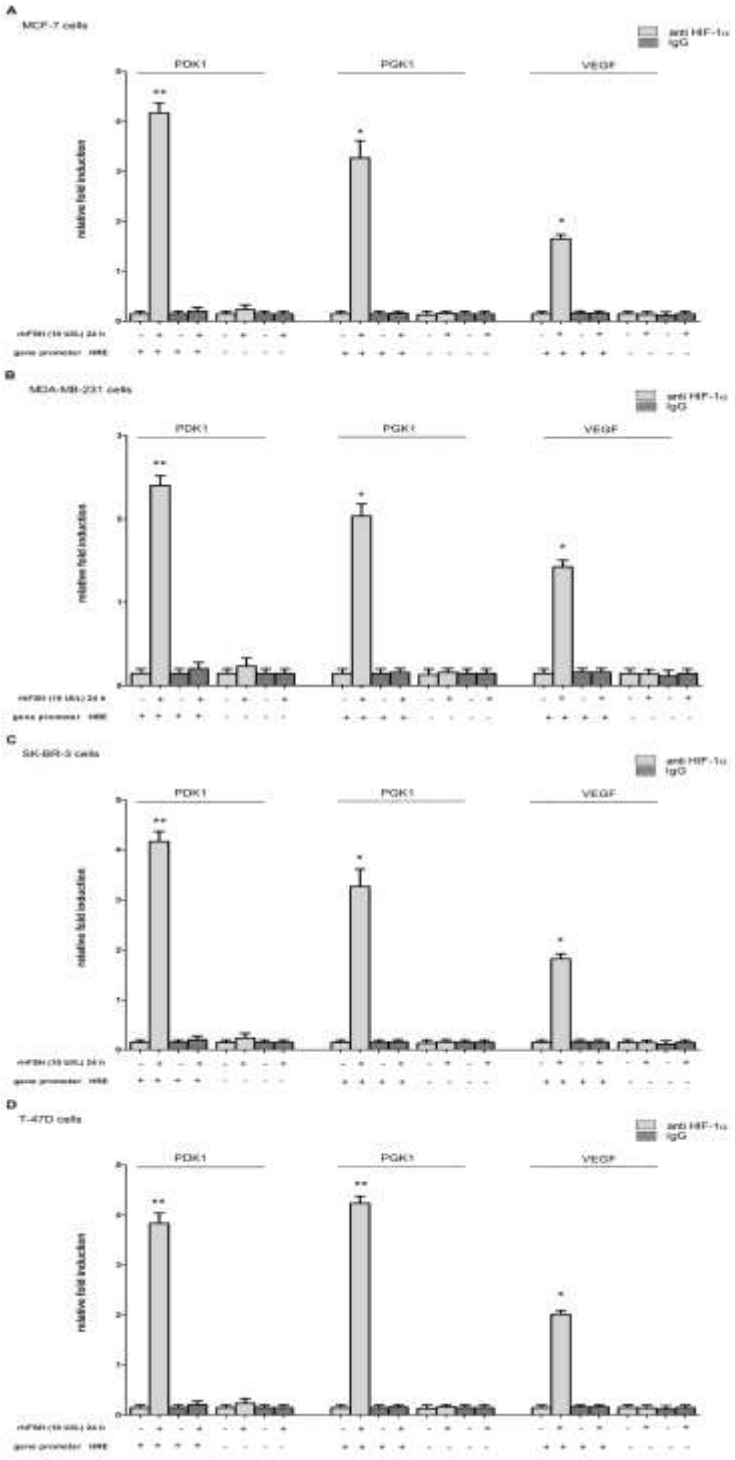

Figure 7. Effect of rhFSH on nuclear HIF-1α activation in human breast cancer cells. The binding of HIF-1α to *PDK1*, *PGK1* and *VEGF* gene promoters after FSH incubation was measured by ChIP assay. RT-PCR analysis for *PDK1*, *PGK1* and *VEGF* promoter region containing (+) or not (-) a HRE was performed on samples immunoprecipitated with anti-HIF-1α antibody (anti-HIF-1α) or IgG (negative control). Measurements (n = 6) were performed in triplicate and repeated two times, and data are presented as means ± SEM. ** $p < 0.0001$ and * $p < 0.001$vs untreated.

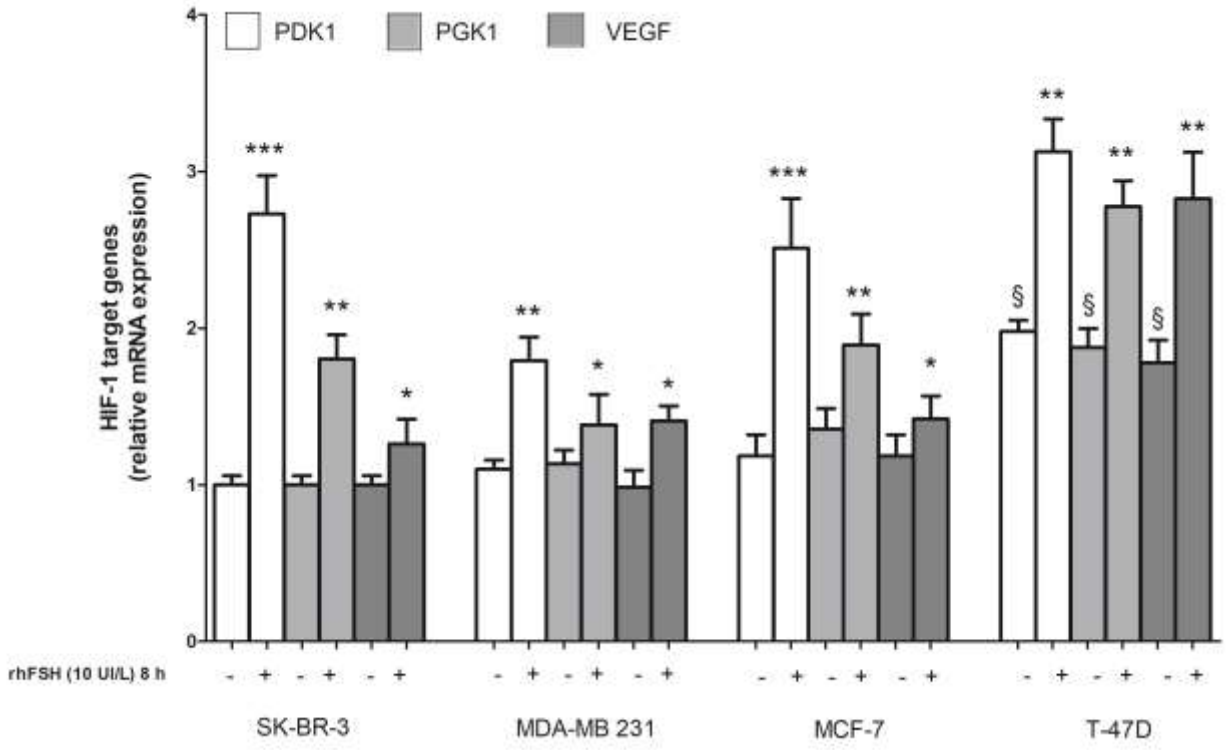

Figure 8. Effect of rhFSH on HIF-1α target genes expression in human breast cancer cells. After 24 h of incubation with FSH the expression of HIF-1α target genes PDK1, PGK1, VEGF was checked by quantitative PCR analysis. The figure is representative of three experiments performed in duplicate. Data are expressed as fold changes versus SKBR3 utreated and are the mean ± SEM. *** p< 0.0001, ** p< 0.001 and * p< 0.01 after rhFSH exposure vs no exposure; § p< 0.001 vs SK-BR-3 untreated.

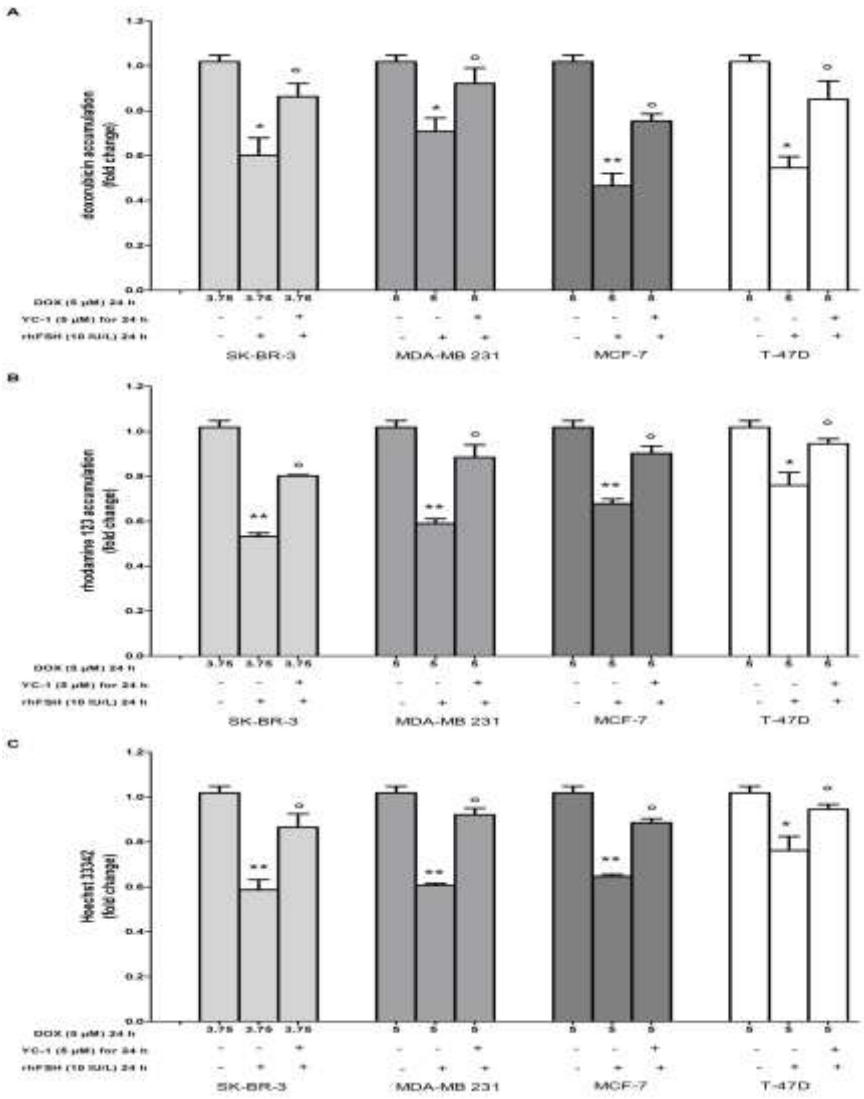

Figure 9. Effect of YC-1, an HIF-1α inhibitor, on the induction of the MDR phenotype triggered by rhFSH in human breast cancer cells. Three assays were carried out after pre-incubation in the absence (-) or in the presence (+) of 5 μM YC-1 for 24 h followed by treatment with rhFSH for 24 h. Measurements were performed in triplicate and repeated two times (n = 6), and data are represented as fold change vs control. (A) DOX accumulation assay was carried out The ATP binding cassette transporters activity was evaluated by intracellular fluorescence of cells exposed to (B) rhodamine 123 (to assess Pgp and MRP activity) or (C) Hoechst 33342 (to assess BCRP activity). The cells were lysed and the intracellular fluorescence, inversely related to fluorescence efflux, was assessed fluorimetrically. Measurements (n = 6) were performed in triplicate and repeated two times. The absorbance values of the treated cells are expressed as fold change versus control. * $p < 0.001$ and ** $p < 0.001$ vs control; ° $p < 0.001$ vs rhFSH alone.